

Received June 26, 2019, accepted July 18, 2019, date of publication July 22, 2019, date of current version August 8, 2019.

Digital Object Identifier 10.1109/ACCESS.2019.2930309

# Holographic Zoom System Having Controllable Light Intensity Without Undesirable Light Based on Multifunctional Liquid Device

DI WANG<sup>1,2</sup>, CHAO LIU<sup>1,2</sup>, AND QIONG-HUA WANG<sup>1,2</sup> 

<sup>1</sup>School of Instrumentation and Opto-electronics Engineering, Beihang University, Beijing 100191, China

<sup>2</sup>Beijing Advanced Innovation Center for Big Data-based Precision Medicine, Beihang University, Beijing 100191, China

Corresponding author: Qiong-Hua Wang (qionghua@buaa.edu.cn)

This work was supported in part by the National Natural Science Foundation of China under Grant 61535007, and in part by the China Postdoctoral Science Foundation under Grant 2019M650422 and Grant 2019M650421.

**ABSTRACT** In this paper, a holographic zoom system having controllable light intensity based on a multifunctional liquid (ML) device is proposed. The system consists of a collimated beam, a PBS, a spatial light modulator (SLM), an ML device, and a receiving screen. Different from the traditional liquid device, the ML device, which consists of the aperture-change part, the focal-length-change part, and the light-intensity-change part, is proposed. The aperture-change part and the focal-length-change part are actuated by the electrowetting effect, and then, the aperture size and the focal length can be changed. In the light-intensity-change part, two polarizers are stuck on the top substrate and the bottom substrate, respectively. By controlling the voltage applied on the liquid crystal cell, the light intensity can be changed easily. When the collimated beam illuminates the SLM, the phase of a spherical wave is loaded on the SLM. By adjusting the radius of the spherical wave and the focal length of the ML device, holographic zoom function can be realized. When diffraction images pass through the ML device, the reconstructed image can be displayed without diffraction beams and high-order diffraction images. Moreover, the size and intensity of the reconstructed image can be adjusted conveniently with such a simple system. The experimental results verify the feasibility of the proposed system.

**INDEX TERMS** Spatial light modulator, liquid device, iris.

## I. INTRODUCTION

Human beings live in a three-dimensional world, where the reception and display of three-dimensional information is an important way for human visual reproduction. With the development of science and technology, people have gradually made breakthroughs in the collection, storage, processing and transmission of three-dimensional information. As one of the true three-dimensional displays, holographic display can completely record and reconstruct the wavefront information of the objects, so it can provide all the depth information needed in human visuals [1]–[4]. Therefore, the holographic display technology has become an important development direction in the field of information display. So far, though the researches of the holographic display have achieved lots of results, there are still many problems that limit its development such as color holographic reconstruction and

undesirable light elimination [5]–[8]. The common way to realize color holographic display is time multiplexing method by using one spatial light modulator (SLM) or spatial multiplexing method by using three SLMs [9]–[11]. Besides, spatial multiplexing method by using an SLM is also proposed to reconstruct the color holographic image in order to simplify the system [12]. In the color holographic reconstruction, people usually pay attention to the precise coincidence of the three colors. But there is still another problem: color intensity matching [13]–[15]. The human eye is different in sensitivity to different colors of light, and the power loss of each laser is different. So, the intensity of each color reproduction image is different, and the color of the reproduced image may differ from the original object accordingly. This kind of reconstructed image with uneven intensity will affect the visual effect. The common way to adjust the laser power is using current control or pulse-width-modulation method. Moreover, the light intensity is affected by the optical path of the system [16]–[18]. Using an optical attenuator in the

The associate editor coordinating the review of this manuscript and approving it for publication was Wen Chen.

holographic system is also an option, but the mechanical operation is not convenient in the experiment. In contrast, researches about eliminating the undesirable light have been studied a lot [19], [20]. In order to eliminate undesirable light that caused by the pixelated structure of the SLM, which is a typical problem when using pixelated SLM for holographic display. Some scholars have proposed to use  $4f$  system in the holographic reconstruction [21]. However, using a  $4f$  system will make the entire holographic system more complicated. Some scholars remove the zero-order noise by loading converging spherical wave to the phase distribution of the hologram [22], then the zero-order noise can be eliminated with a solid aperture. Moreover, techniques by adding linear phase factors have also been proposed to separate the zero-order noise [23]. The desirable holographic system not only needs to use several solid lenses and filters to eliminate the undesirable light, but also needs optical attenuator (such as two half-wave plates) to adjust the light intensity of the reproduction [24]–[26]. However, such systems are very complex. If we want to achieve the zoom function, the system will be more complicated. While the applications of holographic display such as virtual reality and augmented reality often require lightweight features.

Recently, with the development of liquid photonics devices, liquid devices such as liquid lens and liquid aperture have been gradually used in the holographic display system for better reproduction [27]–[32]. The advantages of liquid device are the variable changes with low cost and simple fabrication. So, the liquid device can inject new vitality into the development of the holographic display.

In this paper, a multifunctional liquid (ML) device based on electrowetting effect is proposed and combined with the holographic display system innovatively. Different from the traditional liquid device, the ML device has the functions of controllable light intensity, focal length and aperture size at the same time. By using the ML device in the holographic display system, the intensity and size of the reconstructed image can be adjusted, and the reconstructed image can be displayed without undesirable light with a simple structure. With the optimization of liquid device performance, the holographic display system based on the liquid device can really go to application in the future.

## II. STRUCTURE AND OPERATING PRINCIPLE

The proposed system consists of a collimated beam, a PBS, an SLM, an ML device and a receiving screen, as shown in Fig. 1. The PBS is located between the SLM and the collimated beam. The ML device is located between the BS and the receiving screen. When the collimated beam passes through the PBS and illuminates the SLM, the hologram that is loaded on the SLM is modulated. Then the diffraction light passes through PBS and ML device. By adjusting the voltage applied on the ML device, the reconstructed images can be displayed on the receiving screen. As one of the core components of the system, the ML device is used not only to adjust the light intensity, but also to adjust the field of view.

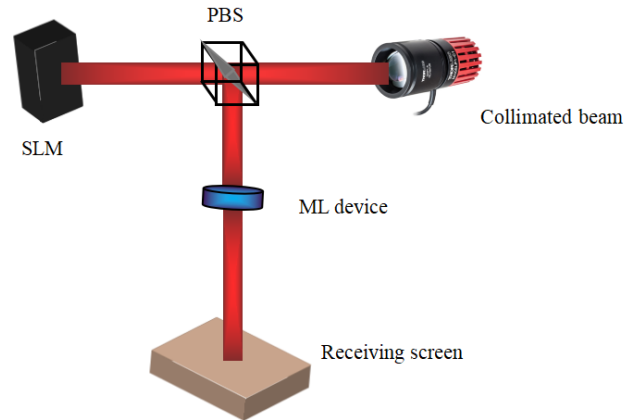


FIGURE 1. Structure of the proposed system.

So, the reconstructed image can be displayed without high-order diffraction images and high-order diffraction beams.

In the holographic reproduction, when the collimated beam illuminates the SLM, the diffraction distribution after the SLM can be expressed as the following formula:

$$U_f(x, y) = \frac{e^{ikf}}{i\lambda f} \exp\left[\frac{i\pi}{f\lambda}(x^2 + y^2)\right] \times \int_{-\infty}^{\infty} \int_{-\infty}^{\infty} [U(u, v)] \exp\left[\frac{-2i\pi}{f\lambda}(xu + yv)\right] dudv, \quad (1)$$

where  $U_f(x, y)$  is the diffraction distribution of the reconstruction,  $k = 2\pi/\lambda$ ,  $f$  is the focal length of the ML device,  $\lambda$  is the wavelength, and  $U(x, y)$  is the distribution of the hologram. When the hologram is loaded on the SLM, the reconstructed image can be reflected on the receiving screen by the PBS. In order to eliminate the undesirable light and realize zoom function, we load a spherical wave (the radius is  $l$ ) on the SLM. As shown in Fig. 2, according to the holographic diffraction theory, the size of the reconstructed image on the receiving screen can be calculated as follows:

$$H = \frac{\lambda f d_2}{p(l + d_1)}, \quad (2)$$

where  $H$  is the size of the reconstructed image,  $d_1$  is the distance between the SLM and the ML device,  $p$  is the pixel pitch of the SLM, and  $d_2$  is the distance between the ML device and the receiving screen. It can be seen clearly that the size of the reconstructed image is determined by  $f$  and  $l$ . So, by changing the focal length  $f$  and the radius  $l$  of the spherical wave, the size of the reconstructed image can be adjusted

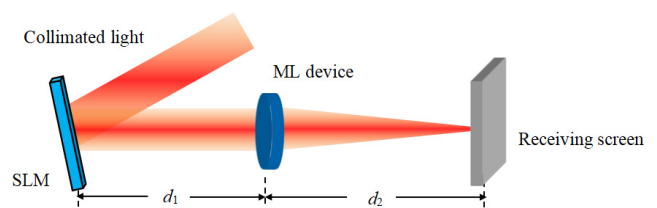
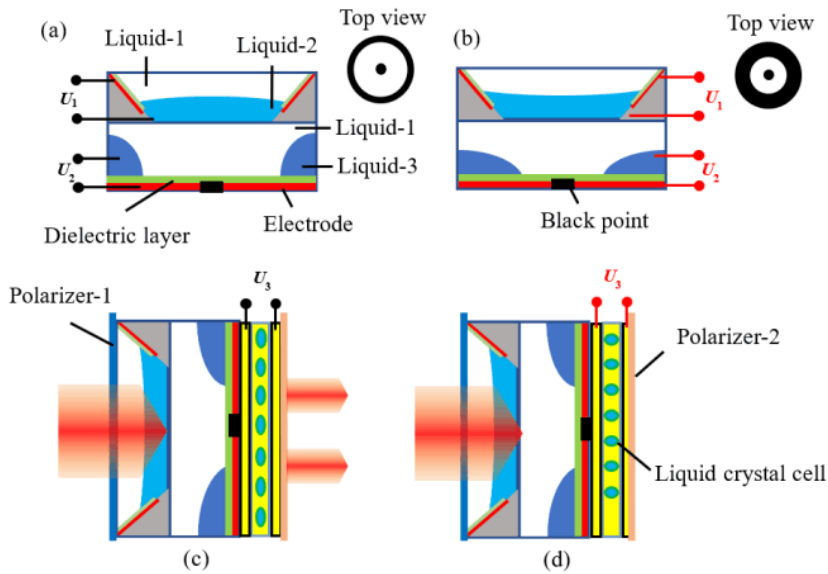


FIGURE 2. Analysis diagram of the proposed system.



**FIGURE 3.** Structure and mechanism of the ML device. (a) Iris and lens without DC voltage; (b) iris and lens with DC voltage; (c) voltage-off state with liquid crystal cell; (d) voltage-on state with liquid crystal cell.

without moving the positions of the optical components in the proposed system. When light passes through the ML device, the diffraction light and the high-order reconstructed images caused by the pixel structure of the SLM can be eliminated by the aperture-change part of the ML device, then the reconstructed image with high quality can be displayed on the receiving screen.

The structure of the proposed ML device is shown in Fig. 3. The ML device consists of three parts: the focal-length-change part, the aperture-change part and light-intensity-change part. Liquid-1, liquid-2 and liquid-3 are the no-conductive liquid, conductive liquid and dyed liquid, respectively. In the focal-length-change part, liquid-1 and liquid-2 are filled in the chamber. When the voltage  $U_1$  is applied on the sidewall electrode, the shape of the liquid-liquid interface will be changed to reach the function of variable focal length change. In the aperture change part, a black shading film is secured to the bottom substrate. When the voltage  $U_2$  is applied on liquid-3 and electrode, liquid-3 rushes into the center of the bottom substrate due to the electrowetting effect. Hence, the aperture sizes can be changed, as shown in Figs. 3(a)-(b). Take the focal-length-part as an example, the relationship between the contact angle  $\theta$  and the applied voltage  $U$  can be described by the following equation:

$$\cos \theta = \frac{\gamma_1 - \gamma_2}{\gamma_{12}} + \frac{\varepsilon}{2\gamma_{12}d}U^2, \quad (3)$$

where  $\varepsilon$  is dielectric constant of the insulating layer,  $d$  is the thickness of the insulating layer,  $\theta$  is the contact angle between liquid-2 and the bottom substrate,  $\gamma_1$ ,  $\gamma_2$ , and  $\gamma_{12}$  are the interfacial tensions between the bottom substrate and liquid-1, the bottom substrate and liquid-2 and the two liquids respectively. The mechanism of the aperture-change part is the same as that of the focal-length-change part.

As for the light-intensity-change part, two polarizers are stuck on the top and bottom substrates, respectively. The liquid crystal (LC) cell is a  $90^\circ$  twisted-nematic (TN) cell and polarizer-1 is orthogonal to polarizer-2. When no voltage is applied on the LC cell, the light beam can pass through the aperture. The incident light can be rotated the polarization by the TN layer with  $90^\circ$ , as shown in Fig. 3(c). When the LC cell is applied on a voltage  $U_3$ , the LC directors are reoriented to be perpendicular to that of the voltage-off state. In this state, the phase of the light beam changes little. Thus, the light aperture shows closed state, as depicted in Fig. 3(d). In this way, the proposed ML device can achieve the function of controlling the focal length, aperture size and light intensity in a system, simultaneously.

In the holographic reconstruction, when light passes through the BS, the result received on the receiving screen consists of the multi-order diffraction images and the multi-order diffraction light caused by the pixel structure of the SLM. By changing the focal length of the ML device and the radius of the spherical wave, the size of the reconstructed image can be adjusted easily. When light passes through the ML device, the size of the reconstructed image can be adjusted according to the needs. The high-order diffraction images and high-order diffraction light can be absorbed by the dyed liquid of the ML lens. So, we can see the ideal reconstructed image on the receiving screen. Besides, by adjusting the voltage applied on the LC cell, the intensity of the reconstructed image can be changed easily. Therefore, the reconstructed image with desirable intensity can be displayed to meet the requirement.

### III. EXPERIMENTS AND RESULTS

In order to verify the feasibility of the proposed system, the ML device is produced. When the voltage applied on the

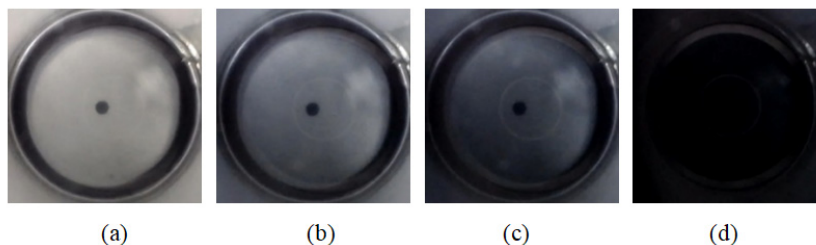


**FIGURE 4.** Results of the intensity change when voltage is applied on the electrode. (a)  $U = 0\text{ V}$ ; (b)  $U = 3\text{ V}$ ; (c)  $U = 4\text{ V}$ ; (d)  $U = 5\text{ V}$ .

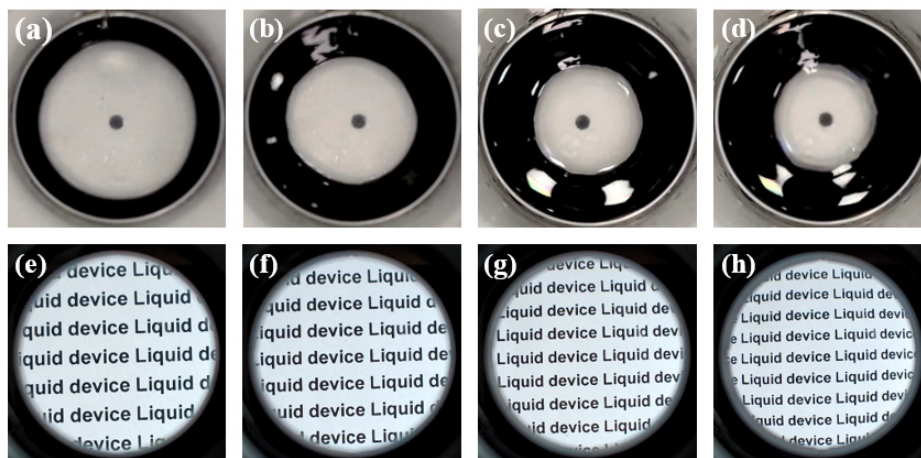


**FIGURE 5.** Results of the aperture size changes and the focal length changes when we apply voltages on the electrode. (a) Aperture result when  $U = 0\text{V}$ ; (b) aperture result when  $U = 50\text{V}$ ; (c) aperture result when  $U = 65\text{V}$ ; (d) aperture result when  $U = 80\text{V}$ ; (e) focal length result when  $U = 0\text{V}$ ; (f) focal length result when  $U = 50\text{V}$ ; (g) focal length result when  $U = 65\text{V}$ ; (h) focal length result when  $U = 80\text{V}$ .

liquid crystal cell changes from 0 V to 5V, the light transmittance changes accordingly, as shown in Fig. 4. A piece of paper full of letters is put under the ML device. As can be seen from the results, the viewing intensity of the letters changes with the voltage.

In this experiment, the phenylmethyl silicone oil (a density of  $\sim 1.03\text{ g/cm}^3$ ) is used as liquid-1, the NaCl solution is used as liquid-2 (the density of the solution is  $\sim 1.03\text{ g/cm}^3$ ), and the propyl alcohol mixed with ink (a density of  $\sim 1.03\text{ g/cm}^3$ ) is used as liquid-3. The size of the iris can be changed by applying voltages on the electrode and liquid-3. A CCD is put on the top of the liquid iris to record the image during actuation process. Figs. 5(a)-(d) shows the aperture changes when different voltages are applied on the iris. In the initial state, liquid-3 is clung to the sidewall of the substrate. The iris shows the largest aperture. The aperture is  $\sim 12.4\text{ mm}$ , as shown Fig. 5(a). In this experiment, the threshold voltage of the proposed iris is  $\sim 35\text{ V}$ . So, when  $U > 35\text{ V}$ , liquid-3 begins to rush to the center. It can be seen clearly that the aperture shrinks when the applied voltage increases from 50V to 80V, as shown in Figs. 5(b)-(d). The measured aperture sizes are 10.9mm, 9.8mm, 9.1mm, 8.4mm and 7.6mm, respectively. Such an experiment shows the aperture sizes can be changed variably. The focal-length-change can be also controlled by applying voltage from 50V to 80V, as shown in Figs. 5(e)-(h). The experiments show that the focal length

can be changed from  $\sim 19\text{cm}$  to  $+\infty$  and  $\sim -93\text{cm}$  to  $-\infty$ . The measured aperture sizes and focal lengths under different applied driving voltages are also depicted in Fig. 6. It can be seen clearly that the aperture size is decreased with the increasing of the voltage. The focal length can be adjusted by controlling the voltage. Besides, the ML device can realize the functions of positive and negative lenses.

In the holographic system, a green laser is used in the experiment and the wavelength is 532nm. An SLM is used as the phase modulator and its specific parameters is shown in Table 1. The distance between the SLM and the ML device is 150mm, and the distance between the ML device and the receiving screen is 300mm. A cup is used as the recorded object, as shown in Fig. 7(a). The Gerchberg-Saxton (GS) algorithm is used in the experiment and the number of iterations is set to 40. Fig. 7(b) is the hologram of the recorded object by using the GS algorithm. In the traditional

**TABLE 1.** Specific parameters of the SLM.

Modulation type	Effective image plane size	Diffraction efficiency	Fill factor
Phase	12.29×6.91mm	75%	>93%



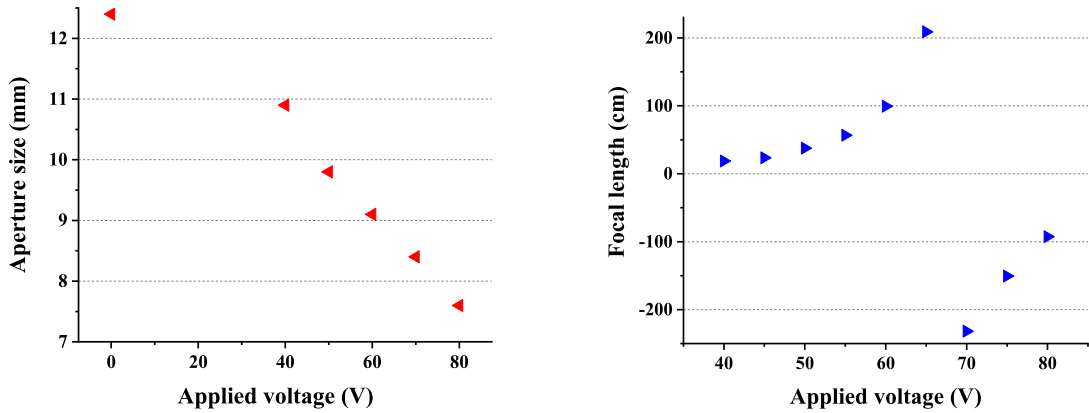


FIGURE 6. Relationship between the aperture size, focal length and the driving voltage.

holographic system, a solid lens is usually used to reconstruct the image. Fig. 7(c) is the result of the reconstructed image by using the traditional holographic system. The result shows that the quality of the reconstructed image is disturbed by the high-order diffraction images and high-order diffraction light. In the proposed system, in order to eliminate the undesirable light, the spherical wave is loaded on the SLM. By adjusting the focal length of the ML device and the radius of the spherical wave, the clear reconstructed image can be seen on the receiving screen. When using the ML device in the system, by adjusting the voltage applied on the electrode and liquid-3, undesirable light in the reconstructed image can be eliminated and the desirable reconstructed image can be displayed on the receiving screen, as shown in Fig. 7(d).

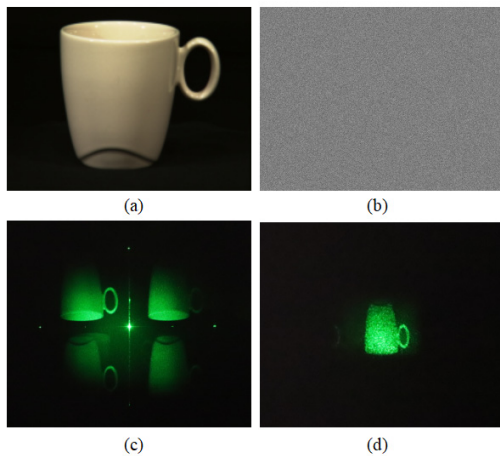


FIGURE 7. Results of the reconstructed images. (a) Recorded object; (b) hologram of the recorded object by using the GS algorithm; (c) reconstructed image of the traditional holographic system without the ML device; (d) reconstructed image of the proposed system.

By changing the voltage of the LC cell, the light intensity of the reconstructed image can be adjusted easily accordingly, as shown in Figs. 8(a)-8(e). Therefore, with the ML device in the system, the holographic display system having controllable light intensity without undesirable light can be realized conveniently.

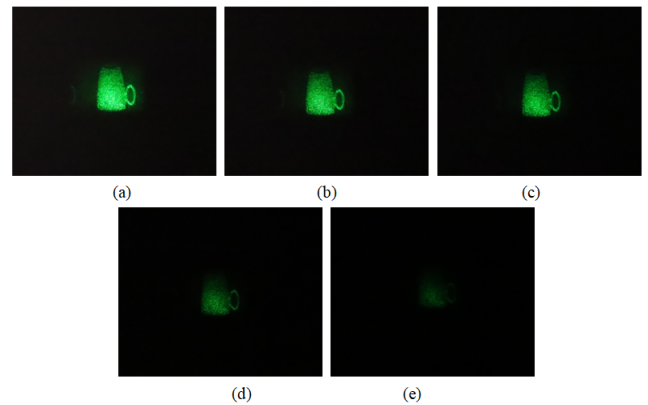


FIGURE 8. (a)-(e) are the reconstructed images with different light intensities.

From Eq. (2) we know that the size of the reconstructed image is determined by the focal length of the ML device and the radius of the spherical wave. When the radius of the spherical wave changes, the size of the reconstructed image on the receiving screen can be adjusted accordingly by controlling the voltage applied on liquid-2. In this way, holographic zoom system can be realized easily without moving any optical components in the system. We define the magnification of the system to be 1 when the radius value is 55cm. For different sizes of the reproduced images, high-quality reproduction can be easily achieved by changing the aperture-change part of the ML device, as shown in Fig. 9. In the experiment, the position of the optical components is fixed, and the size of the ML device is only a few centimeters.

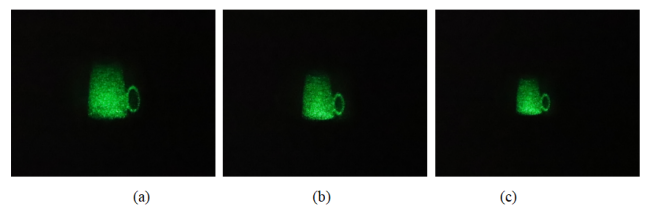


FIGURE 9. (a)-(c) are the reconstructed images with different sizes. (a)  $M = 1.6$ ; (b)  $M = 1.3$ ; (c)  $M = 1$ .

Compared with the existing technology, the proposed system has the following differences and advantages. Compared with our previous work of Ref. [23], the driving principle of the two liquid devices are different. The liquid device of Ref. [23] is based on hydrodynamic actuation. By changing the volume of the black droplet injected into the chamber, the aperture size can be adjusted accordingly. While the ML device is based on electrowetting effect. Therefore, they are two devices with different principles and structures. The liquid device of Ref. [23] can only implement the function of the variable aperture, while the ML device has the functions of controllable light intensity, focal length and aperture size at the same time. Therefore, the ML device has greater advantages in structure and performance than the previous device. The ML device based electrowetting effect has advantages such as fast response time, and it may be applied to the holographic real-time display in the future. The response time of the LC cell is shown in Fig. 10. With such a device, the controllable holographic zoom system without undesirable light can be realized with a fast response time. The holographic system of the previous work can only eliminate the undesirable light. When the size of the reconstructed image changes, the position of the receiving screen will be changed. If we want to achieve the zoom effect, additional solid lens groups or zoom lenses are needed. While in the proposed system, the size and intensity of the reconstructed image can be adjusted simultaneously without moving any optical element position. Therefore, the proposed system has greater advantages in performance and structure than the previous system. Moreover, the traditional method is using two polarizers to adjust the light intensity of the holographic reproduction. Besides, the traditional method of eliminating the undesirable light in the reconstructed image is using several solid lenses and filters. So, the system will become more complex if the zoom function is to be achieved. The advantage of the proposed system is the multifunctional integration of the liquid device. The ML device integrates the functions of the lens, the diaphragm and the optical attenuation. The LC-based attenuators have the advantages of fast response time and low

driving voltage. Besides, these devices are simple to fabricate and easy to integrate. The size of the whole ML device is only a few centimeters. Because the liquid device has the advantages of small size, ease of integration and precise control, the holographic system can be highly simplified. That is also the key novelty of the proposed system.

To date, color-matched holographic display effect based on the simple system is difficult to achieve. When the ML device is used in the color holographic system, the color of the reproduced image can be adjusted more realistically, and the effect of the color holographic display will be greatly improved. However, there are still some problems in the proposed system. In the holographic reconstruction, due to the elimination of the undesirable light, the intensity of the reconstructed image is greatly decreased. On the other hand, the propagation of the light path and the absorption of the liquid also affect the intensity of the reconstructed image. At present, the improvement of the diffraction efficiency is one of the problems to be solved in the holographic display application. Due to the absorption characteristics of the liquid itself and the LC cell, the transmittance is affected. In addition, the aperture shapes are irregular when the driving voltage raises to 50V and 80V, as shown in Fig. 5(c) and Fig. 5(d) respectively. That may result from the simple structure of the ITO substrate which has no limitation to the liquid when the liquid stretches into the center. We can design an annular ITO electrode to make the liquid flow into the center regularly. In the experiment, the spherical wave is used to separate the diffraction beams and the reconstructed image.

#### IV. CONCLUSION

In this paper, a new ML device is combined with the holographic display system is proposed innovatively. The ML device with adjustable light intensity, controlled focal length and aperture size based on electrowetting is proposed. By using the ML device in the holographic display system, the size and intensity of the reconstructed image can be adjusted, and the reconstructed image can be displayed without undesirable light. The proposed system has a simple structure. Maybe, with the performance optimization of liquid device, the holographic display system based on the liquid device can really go to application in the future.

#### REFERENCES

- [1] L. Wang, S. Kruk, H. Tang, T. Li, I. Kravchenko, D. N. Neshev, and Y. S. Kivshar, "Grayscale transparent metasurface holograms," *Optica*, vol. 3, no. 12, pp. 1504–1505, 2016.
- [2] Z. L. Deng, J. Deng, X. Zhuang, S. Wang, T. Shi, G. P. Wang, Y. Wang, J. Xu, Y. Cao, X. Wang, X. Cheng, G. Li, and X. Li, "Facile metagrating holograms with broadband and extreme angle tolerance," *Light Sci. Appl.*, vol. 7, p. 78, Oct. 2018.
- [3] Y. Sando, K. Satoh, T. Kitagawa, M. Kawamura, D. Barada, and T. Yatagai, "Super-wide viewing-zone holographic 3D display using a convex parabolic mirror," *Sci. Rep.*, vol. 8, p. 11333, Jul. 2018.
- [4] H. Yu, K. Lee, J. Park, and Y. Park, "Ultrahigh-definition dynamic 3D holographic display by active control of volume speckle fields," *Nature Photon.*, vol. 11, pp. 186–192, Jan. 2017.
- [5] B. J. Jackin and T. Yatagai, "Fast calculation of spherical computer generated hologram using spherical wave spectrum method," *Opt. Express*, vol. 21, no. 1, pp. 935–948, 2013.

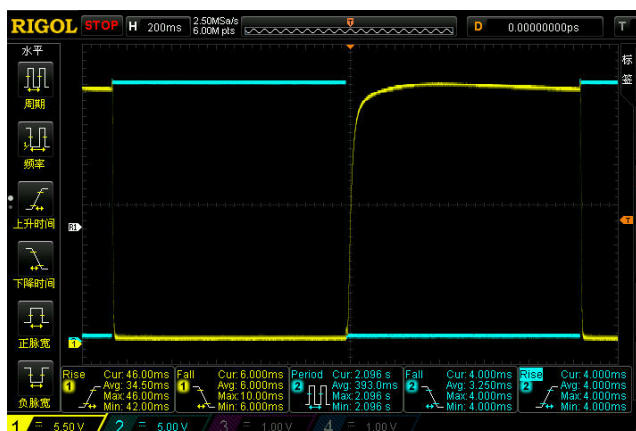


FIGURE 10. Response time of the LC cell.

- [6] J. S. Lee, Y. K. Kim, M. Y. Lee, and Y. H. Won, "Enhanced see-through near-eye display using time-division multiplexing of a Maxwellian-view and holographic display," *Opt. Express*, vol. 27, no. 2, pp. 689–701, 2019.
- [7] Y.-L. Piao, M.-U. Erdenebat, K.-C. Kwon, S.-K. Gil, and N. Kim, "Chromatic-dispersion-corrected full-color holographic display using directional-view image scaling method," *Appl. Opt.*, vol. 58, no. 5, pp. A120–A127, 2019.
- [8] W. Zaperty, T. Kozacki, and M. Kujawińska, "Multi-SLM color holographic 3D display based on RGB spatial filter," *J. Display Technol.*, vol. 12, no. 12, pp. 1724–1731, 2016.
- [9] M. Oikawa, T. Shimobaba, T. Yoda, H. Nakayama, A. Shiraki, N. Masuda, and T. Ito, "Time-division color electroholography using one-chip RGB LED and synchronizing controller," *Opt. Express*, vol. 19, no. 13, pp. 12008–12013, 2011.
- [10] T. Kozacki and M. Chlipala, "Color holographic display with white light LED source and single phase only SLM," *Opt. Express*, vol. 24, no. 3, pp. 2189–2199, 2016.
- [11] F. Yaraş, H. Kang, and L. Onural, "Circular holographic video display system," *Opt. Express*, vol. 19, no. 10, pp. 9147–9156, 2011.
- [12] Y. Tsuchiyama and K. Matsushima, "Full-color large-scaled computer-generated holograms using RGB color filters," *Opt. Express*, vol. 25, no. 3, pp. 2016–2030, 2017.
- [13] H. Mukawa, K. Akutsu, I. Matsumura, S. Nakano, T. Yoshida, M. Kuwahara, and K. Aiki, "A full-color eyewear display using planar waveguides with reflection volume holograms," *J. Soc. Inf. Display*, vol. 17, no. 3, pp. 185–193, 2009.
- [14] M.-L. Piao and N. Kim, "Achieving high levels of color uniformity and optical efficiency for a wedge-shaped waveguide head-mounted display using a photopolymer," *Appl. Opt.*, vol. 53, no. 10, pp. 2180–2186, 2014.
- [15] J.-A. Piao, G. Li, M.-L. Piao, and N. Kim, "Full color holographic optical element fabrication for waveguide-type head mounted display using photopolymer," *J. Opt. Soc. Korea*, vol. 17, no. 3, pp. 242–248, 2013.
- [16] M. Kumar, C. Xia, X. Ma, V. V. Alexander, M. N. Islam, F. L. Terry, Jr, C. C. Aleksoff, A. Klooster, and D. Davidson, "Power adjustable visible supercontinuum generation using amplified nanosecond gain-switched laser diode," *Opt. Express*, vol. 16, no. 9, pp. 6194–6201, 2008.
- [17] S. Smirnov, S. Kobtsev, A. Ivanenko, A. Kokhanovskiy, A. Kemmer, and M. Gervaziev, "Layout of NALM fiber laser with adjustable peak power of generated pulses," *Opt. Lett.*, vol. 42, no. 9, pp. 1732–1735, 2017.
- [18] L. Goldberg, C. McIntosh, and B. Cole, "VCSEL end-pumped passively Q-switched Nd: YAG laser with adjustable pulse energy," *Opt. Express*, vol. 19, no. 5, pp. 4261–4267, 2011.
- [19] T. Senoh, T. Mishina, K. Yamamoto, R. Oi, and T. Kurita, "Viewing-zone-angle-expanded color electronic holography system using ultra-high-definition liquid crystal displays with undesirable light elimination," *J. Display Technol.*, vol. 7, no. 7, pp. 382–390, Jul. 2011.
- [20] D. Wang, C. Liu, C. Shen, X. Zhou, and Q.-H. Wang, "A holographic zoom system without undesirable light," *Optik*, vol. 127, no. 19, pp. 7782–7787, 2016.
- [21] H. Zhang, J. Xie, J. Liu, and Y. Wang, "Elimination of a zero-order beam induced by a pixelated spatial light modulator for holographic projection," *Appl. Opt.*, vol. 48, no. 30, pp. 5834–5841, 2009.
- [22] H.-C. Lin, N. Collings, M.-S. Chen, and Y.-H. Lin, "A holographic projection system with an electrically tuning and continuously adjustable optical zoom," *Opt. Express*, vol. 20, no. 25, pp. 27222–27229, 2012.
- [23] D. Wang, C. Liu, L. Li, X. Zhou, and Q.-H. Wang, "Adjustable liquid aperture to eliminate undesirable light in holographic projection," *Opt. Express*, vol. 24, no. 3, pp. 2098–2105, 2016.
- [24] S. Schuhladen, K. Banerjee, M. Stürmer, P. Müller, U. Wallrabe, and H. Zappe, "Variable optofluidic slit aperture," *Light Sci. Appl.*, vol. 5, Jan. 2016, Art. no. e16005.
- [25] A. Doblas, D. Hincapie-Zuluaga, G. Saavedra, M. Martínez-Corral, and J. Garcia-Sucerquia, "Physical compensation of phase curvature in digital holographic microscopy by use of programmable liquid lens," *Appl. Opt.*, vol. 54, no. 16, pp. 5229–5233, 2015.
- [26] X. Xiang, J. Kim, and M. J. Escuti, "Far-field and Fresnel liquid crystal geometric phase holograms via direct-write photo-alignment," *Crystals*, vol. 7, no. 12, p. 383, 2017.
- [27] C. G. Tsai and J. A. Yeh, "Circular dielectric liquid iris," *Opt. Lett.*, vol. 35, no. 14, pp. 2484–2486, 2010.
- [28] H. Ren, S. Xu, and S.-T. Wu, "Optical switch based on variable aperture," *Opt. Lett.*, vol. 37, no. 9, pp. 1421–1423, 2012.
- [29] C. U. Murade, J. M. Oh, D. van den Ende, and F. Mugele, "Electrowetting driven optical switch and tunable aperture," *Opt. Express*, vol. 19, no. 16, pp. 15525–15531, 2011.
- [30] J. Lee, Y. Park, and S. K. Chung, "Multifunctional liquid lens for variable focus and aperture," *Sens. Actuators A, Phys.*, vol. 287, no. 1, pp. 177–184, 2019.
- [31] C. Liu and D. Wang, "Light intensity and FOV-controlled adaptive fluidic iris," *Appl. Opt.*, vol. 57, no. 18, pp. D27–D31, 2018.
- [32] J.-H. Chang, K.-D. Jung, E. Lee, M. Choi, S. Lee, and W. Kim, "Variable aperture controlled by microelectrofluidic iris," *Opt. Lett.*, vol. 38, no. 15, pp. 2919–2922, 2013.



**DI WANG** is currently a Postdoctoral Research Fellow of optics with the School of Instrumentation and Opto-electronics Engineering, Beihang University. She has published more than 40 papers. Her recent research interest includes information display technologies.



**CHAO LIU** is currently a Postdoctoral Research Fellow of instrumentation with the School of Instrumentation and Opto-electronics Engineering, Beihang University. He has published more than 40 papers. His recent research interests include optical system design, liquid lens, and information displays.



**QIONG-HUA WANG** received the M.S. and Ph.D. degrees from the University of Electronic Science and Technology of China (UESTC), in 1995 and 2001, respectively. She was with UESTC, from 1995 to 2001. She was a Postdoctoral Research Fellow with the School of Optics/CREOL, University of Central Florida, from 2001 to 2004. She was a Professor with the School of Electronics and Information Engineering, Sichuan University, from 2004 to 2018. She is currently a Professor of optics with the School of Instrumentation and Opto-electronics Engineering, Beihang University. She has published approximately 200 papers cited by Science Citation Index and has authored two books. She holds five U.S. patents and 100 Chinese patents. Her research interests include optics and optoelectronics, especially display technologies. She is a Fellow of the Society for Information Display and an Associate Editor of *Optics Express* and the *Journal of the Society for Information Display*.

• • •